# Electronic Supplementary Information

# Thermal properties of lipid bilayers derived from the transient heating regime of upconverting nanoparticles

Ana R. N. Bastos,[a] Carlos D.S. Brites,[a] Paola A. Rojas-Gutierrez,[b] Rute A.S. Ferreira,[a] Ricardo L. Longo, [c*] Christine DeWolf,[b] John A. Capobianco,[b *] and Luís D. Carlos[a*]

[a] Phantom-g, CICECO - Aveiro Institute of Materials, Department of Physics, University of Aveiro, 3810-193, Aveiro, Portugal

[b] Department of Chemistry and Biochemistry, and Centre for NanoScience Research, Concordia University, 7141 Sherbrooke St. West, Montreal, Quebec, H4B 1R6, Canada

[c] Departamento de Química Fundamental, Universidade Federal de Pernambuco, Cidade Universitária, 50740-560, Recife, PE, Brazil

**Table of Contents**

## I. Determination of properties of the UCNPs and nanofluids

The absorption coefficient, $\alpha_J$ (in $m^{-1}$), of an absorbing species J in the (nano)fluid is

$$\alpha_J = (\ln 10)\frac{A_J}{L}$$

where $A_J$ is the absorbance of species J at 980 nm using the solvent as the reference and $L$ is the optical pathlength.

The absorption cross-section, $\sigma_J$ (in $m^2$), of a single absorber J in solution is

$$\sigma_J = \frac{\alpha_J}{N_J}$$

$N_J$ is the number density of J-th absorbers in (number of absorbers-J) $m^{-3}$.

For a solution of absorbers with concentration $C_J$ (in $mg/mL = mg\ cm^{-3}$), $N_J$ is

$$N_J(\#absorbers\ m^{-3}) = \frac{C_J}{m_J} \times 10^6$$

where $m_J$ (in $mg$) is the mass of the absorber-J.

For a pure substance, like the solvent, the absorption cross-section, $\sigma_S$, is

$$\sigma_S = \frac{\alpha_S}{N_S} = \frac{\alpha_S M_S}{\rho_S N_A}$$

where $\alpha_S$, $N_S$, $M_S$, and $\rho_S$ are the absorption coefficient (in $m^{-1}$), the number density in #S $m^{-3}$, the molar mass in $kg\ mol^{-1}$, and the mass density $kg\ m^{-3}$, of the substance and $N_A$ is the Avogadro constant in $mol^{-1}$.

The molar mass of a nanoparticle with composition $LiYF_4$:$Er^{3+}$ $y$%/$Yb^{3+}$ $x$% represented as $LiY_{1-x-y}Yb_xEr_yF_4$, is:

$$M_P = [M_{Li} + (1-x-y)M_Y + yM_{Yb} + xM_{Er} + 4M_F] \times 10^{-3}\ kg\ mol^{-1}$$

where $M_X$ is the atomic molar mass (in $g\ mol^{-1}$) of element $X$.

Given the UCNPs have a square (or tetragonal) bipyramid shape with small diagonal, $d_s$, and long diagonal $d_l$, its volume, $V_P$, is

$$V_P = \frac{1}{6} d_s^2 d_l$$

The mass of one UCNP, $^{m_P}$, is

$$m_P = \rho_{LiYF_4} V_P \frac{M_P}{M_{LiYF_4}}$$

where $^{\rho_{LiYF_4}}$ is the mass density (in $^{kg\,m^{-3}}$) of the undoped NP, which is assumed to be the same as the bulk $^{LiYF_4(s)}$, $^{M_{LiYF_4}}$ is the molar mass, in $^{kg\,mol^{-1}}$, of undoped NPs, and it is assumed that the average volume of the undoped NPs, $^{V_{LiYF_4}}$, is the same as that of doped NPs, $^{V_P}$.

The number of UCNPs, $^{N_{P,b}}$, and of solvent molecules, $^{N_{S,b}}$, exposed to the laser beam are

$$N_{P,b} = N_p A_b L,\ N_{S,b} = N_S A_b L$$

where $^{N_P}$ (in $^{\#NPs\,m^{-3}}$) is the number density of NPs, $^{N_S}$ (in $^{\#S\,m^{-3}}$) is the number density of solvent, $^{A_b}$ (in $^{m^2}$) is the area of the laser spot, and $^{L}$ (in $^{m}$) is the optical pathlength.

## II. Transient heating curves of UCNPs

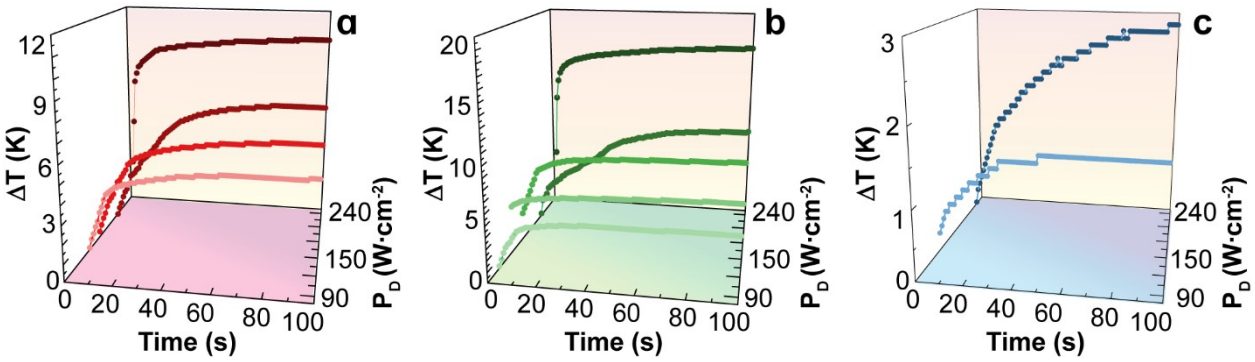


**Figure S1.** Transient heating curves recorded by the immersed thermocouple in (a) lipid bilayer-capped and (b) uncapped UCNPs in $H_2O$, and (c) uncapped UCNPs in $D_2O$.

## III. Determination of the laser power density

To calculate the laser power density, the optical power ($P_L$) and the beam profile were measured by placing a power meter (FieldMaxII-TOP OP-2 Vis, Coherent) and a CCD camera (BC106N-VIS/M, Thorlabs), respectively, at the same position where the sample will be placed during all measurements. Through the 2D projection of the beam profile (inset of Fig. **S2**), the intensity at each pixel was correlated to the measured optical power and divided by the pixel area (6.45×6.45 μm$^2$). An average laser power density ($P_D$) was computed considering only values higher than 36.8%, corresponding to 1/e cut-off value for Gaussian beams (Fig. **S2**).

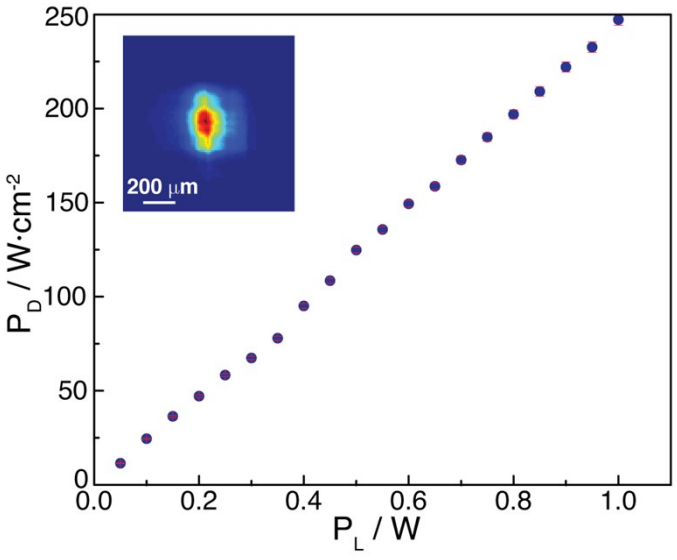


**Figure S2.** Laser power density as a function of the laser power as defined in the laser control software. The inset corresponds to the 2D projection of the beam profile for a laser power density of 125 W·cm$^{-2}$.

## IV. Power gain via absorption

According to the Beer-Lambert law, the transmitted intensity $I$ or radiant power $P$ (in $W$) is

$$I = I_0 e^{-\alpha_N L} \rightarrow P_D = P_{D,0} e^{-\alpha_N L}$$

where the power density $P_D \equiv \frac{I}{A_b} = \frac{P}{A_b}$ (in $W\,m^{-2}$) is the intensity or radiant power divided by the area of the laser beam spot, $A_b$, and $\alpha_N$ (in $m^{-1}$) is the absorption coefficient of the nanofluid. The differential of this attenuation ($\alpha_N > 0$) law is

$$dP_D = -\alpha_N P_D dx$$

or

$$\frac{dP_D}{dx} = -\alpha_N P_D = \frac{d\langle P\rangle}{dV} \equiv -\frac{dW_{abs}}{dV}$$

is the infinitesimal net power lost, $d\langle P\rangle$ (in $W$), by the laser beam per unit volume, $dV$ (in $m^3$), which due to conservation of energy should be the power gained by the nanofluid, $dW_{abs}$ (in $W$), due to absorption. Thus, the infinitesimal power absorbed from the laser beam is

$$dW_{abs} = \alpha_N P_D dV_b = A_b \alpha_N P_D dx = A_b \alpha_N P_{D,0} e^{-\alpha_N x} dx$$

where $dV_b = A_b dx$ is the element of volume of the excitation cylinder of laser beam travelling an infinitesimal pathlength $dx$. The total power absorbed for a pathlength $L$ is

$$W_{abs} = A_b \alpha_N P_{D,0} \int_0^L e^{-\alpha_N x} dx = A_b \alpha_N P_{D,0} \left( -\frac{1}{\alpha_N} e^{-\alpha_N x} \Big|_0^L \right) = \left(1 - e^{-\alpha_N L}\right) A_b P_{D,0}$$

In summary, the power, $W_{abs}$ (in $W$), absorbed from the laser beam is

$$W_{abs} = \left(1 - e^{-\alpha_N L}\right) A_b P_D \cong \alpha_N L A_b P_D = (N_{P,b}\sigma_P + \sigma_{S,b}) P_D$$

where $\alpha_N$ is the absorption coefficient (in $m^{-1}$) of the nanofluid, $A_b$ (in $m^2$) is the spot area, $P_D$ (in $W\,m^{-2}$) is the incident power density, $N_{P,b}$ is the number of NPs exposed to the laser beam,

$\sigma_P$ is the absorption cross-section of one NP, and $\sigma_{S,b}$ is the absorption cross-section of the solvent within the laser beam.

## V. Heat dissipation and power balance equation

The laser beam can be considered as a long excitation cylinder because the optical pathlength is much larger (ca. 100 times) than the diameter of the laser spot. So, the heat absorbed from the laser beam will be dissipated through the surface, $A_{cs}$, of the excitation cylinder.

***Power dissipation via heat transfer***

According to Fourier's law of heat conduction,[1] the rate of heat dissipation by conduction, $W_{cond}$ (in $W$), due to a temperature gradient is

$$W_{cond}(t) = A_{cs}\kappa_m \frac{\partial T(r,t)}{\partial r}$$

where $A_{cs}$ (in $m^2$) is the cross-sectional area of the heat flux, $\kappa_m$ (in $W\,m^{-1}\,K^{-1}$) is the thermal conductivity of the medium, and $\frac{\partial T(r,t)}{\partial r}$ is the temperature gradient. For a small temperature difference, $\Delta T(t)$, between the excitation cylinder and the surrounding fluid, the differential form of the temperature gradient can be approximated by its finite difference form, namely,

$$\frac{\partial T(r,t)}{\partial r} \cong \frac{T(t) - T_0}{r - r_0} = \frac{\Delta T(t)}{\Delta r}$$

where $\Delta r$ is a radial distance for which the temperature decreases from $T(t)$ to room temperature $T_0$ and spatial homogeneity was assumed. So, the rate of heat dissipation by conduction becomes

$$W_{cond}(t) \cong A_{cs}\kappa_m \frac{\Delta T(t)}{\Delta r} = A_{cs}h_{cond}\Delta T(t),\ h_{cond} = \frac{\kappa_m}{\Delta r}$$

where $h_{cond}$ (in $W\,m^{-2}\,K^{-1}$) is the thermal conduction coefficient and thermal conductivity $\kappa_m$ was considered to be independent of the temperature.

A heated region can also cool-down via convection. According to Newton's cooling law the convective heat dissipation, $W_{conv}(t)_1$, by the laser heated nanofluid is

$$W_{conv}(t) = A_{cs}h_{conv}\Delta T(t)$$

where $h_{conv}$ (in $W\,m^{-2}\,K^{-1}$) is the convection heat transfer coefficient. A convection process can usually be classified as free, forced, and phase change (e.g. boiling or condensation).

The matter at a temperature above 0 K emits thermal radiation with an upper limit to its emissive power, $E_{bb}$, given by the Stefan-Boltzmann law,

$$E_{bb} = \sigma_{SB}A_{cs}T^4$$

where $\sigma_{SB}$ (in $W\,m^{-2}\,K^{-4}$) is the Stefan-Boltzmann constant, $A_{cs}$ (in $m^2$) is the cross-sectional area of the heat flux, and $T$ is the temperature of the blackbody. For a body that is not a perfect emitter, its emissive power, $E_b$, is

$$E_b = \varepsilon\sigma_{SB}A_{cs}T^4$$

where $0 \leq \varepsilon \leq 1$ the emissivity of the body. If the surroundings of this body are at a lower and constant temperature $T_0$, then it behaves as an emitter at this temperature and by energy conservation, this emitted thermal radiation is absorbed by the surface area, $A_{cs}$, of the body. As a result, there will be a net power dissipation, $W_{rad}(t)$, from the heated region of the nanofluid given by

$$W_{rad}(t) = E_b - E_{abs} = \varepsilon\sigma_{SB}A_{cs}T^4(t) - \varepsilon\sigma_{SB}A_{cs}T_0^4 = \varepsilon\sigma_{SB}A_{cs}\left[T^4(t) - T_0^4\right]$$

This expression can be recast into

$$W_{rad}(t) = h_{rad}A_{cs}\Delta T(t)$$

where the thermal radiation coefficient $h_{rad}$ (in $W\,m^{-2}\,K^{-1}$) can be expressed as

$$h_{rad} = \varepsilon\sigma_{SB}\left[T(t) + T_0\right]\left[T^2(t) + T_0^2\right]$$

because

$$[T(t)+T_0]\left[T^2(t)+T_0^2\right]\Delta T(t) = \left[T^3(t)+T(t)T_0^2+T^2(t)T_0+T_0^3\right][T(t)-T_0] = T^4(t)+T^2(t)T_0^2+T^3(t)T_0+T(t)T_0^3-T^3(t)$$
$$T_0-T(t)T_0^3-T^2(t)T_0^2-T_0^4 = T^4(t)-T_0^4$$

At near room temperature $T_0 = 300\ K$ and a temperature increase $\Delta T = 10\ K$, *i.e.* $T(t) = 310\ K$, the thermal radiation coefficient $h_{rad}$ (in $W\ m^{-2}\ K^{-1}$) can

$$h_{rad} = \varepsilon\sigma_{SB}[T(t)+T_0]\left[T^2(t)+T_0^2\right] = \varepsilon(5.670374419\times10^{-8}\ W\ m^{-2}\ K^{-4})(1.1352\ W\ m^{-2}\ K^{-1}$$

It is noteworthy that all three contributions to the heat transfer dissipation have the same functional form, so they can be combined into a general expression for the power loss via heat transfer

$$W_{ht}(t) = h_{ht}A_{cs}\Delta T(t)$$

where the heat transfer coefficient $h_{ht}$ (in $W\ m^{-2}\ K^{-1}$) is a combination of the conduction, convection and thermal radiation coefficients.

***Power dissipation via upconversion emission***

The UCNPs in the nanofluid absorb radiation from the laser at near-infrared wavelength and emit radiation in the visible region. This process will then decrease the amount of absorbed energy that is transformed into heat, so it will not contribute to the heating of the nanofluid and can be accounted as dissipated power.

The quantum yield, $\phi_{UC}$, of the UC processes is given by the ratio of the number of photons emitted, $N_{ph}^{em}$, to the number of photons absorbed, $N_{ph}^{abs}$,

$$\phi_{UC} = \frac{N_{ph}^{em}}{N_{ph}^{abs}}$$

So, the emitted energy is $E_{em} = N_{ph}^{em} h\nu_{em}$, where $h$ (in $J\,Hz^{-1}$) is the Planck constant and $\nu_{em}$ (in $Hz$) is the frequency of the emission and similarly for the absorbed energy: $E_{abs} = N_{ph}^{abs} h\nu_{abs}$ at frequency $\nu_{abs}$. As a result, the UC quantum yield becomes

$$\phi_{UC} = \frac{N_{ph}^{em} h\nu_{em}\, c\nu_{abs}}{N_{ph}^{abs} h\nu_{abs}\, c\nu_{em}} = \frac{E_{em}\tilde{\nu}_{abs}}{E_{abs}\tilde{\nu}_{em}}$$

where $c$ (in $cm\,s^{-1}$) is the speed of light, $\tilde{\nu}_{abs}$ (in $cm^{-1}$) and $\tilde{\nu}_{em}$ (in $cm^{-1}$) are the absorption and emission wavenumbers. In a given time interval, $\Delta t$:

$$\phi_{UC} = \frac{E_{em}/\Delta t\tilde{\nu}_{abs}}{E_{abs}/\Delta t\tilde{\nu}_{em}} = \frac{W_{UC}\ \ \tilde{\nu}_{abs}}{W_{UC,abs}\tilde{\nu}_{em}}$$

where $W_{UC}$ is the radiative emitted power and $W_{UC,abs}$ is the absorbed power during the UC process. Therefore,

$$W_{UC} = \frac{\tilde{\nu}_{em}}{\tilde{\nu}_{abs}}\phi_{UC} W_{UC,abs} = \frac{\tilde{\nu}_{em}}{\tilde{\nu}_{abs}}\phi_{UC} N_{P,b}\sigma_P P_D$$

where $N_{P,b}$ is the number of UCNPs within the laser beam and $\sigma_P$ is the absorption cross-section of the NPs.

For the uncapped and lipid bilayer-capped $LiYF_4:Yb^{3+}/Er^{3+}$ UCNPs employed as the nanofluids, the ratio of the wavenumbers is $\tilde{\nu}_{em}/\tilde{\nu}_{abs} \cong 0.5$ (two-photon upconversion) and the upconversion quantum yields for these UCNPs dispersed in water are $(0.040\pm0.004)\times10^{-4}$ and $(0.120\pm0.010)\times10^{-4}$, respectively. Therefore,

$$W_{UC} \lesssim 5\times10^{-5} N_{P,b}\sigma_P P_D$$

which results in,

$$\frac{W_{UC}}{W_{abs}} \sim \frac{5\times10^{-5} N_{P,b}\sigma_P P_D}{(N_{P,b}\sigma_P + \sigma_{S,b})P_D} \lesssim 10^{-5}$$

***Heat dissipation via increase of internal energy***

Because the nanofluid within and surrounding the excitation cylinder of the laser beam has heat capacity, $^{c_N}$, it can store energy and the rate of energy storage or the rate of internal energy increase, $^{W_{int}(t)}$, is

$$W_{int}(t) = m_N c_N \frac{dT(t)}{dt}$$

where $^{m_N}$ (in $kg$) is the mass of the nanofluid and $^{c_N}$ (in $J\,K^{-1}\,kg^{-1}$) is the heat capacity of the region where the temperature is increasing. Assuming that the species constituting the nanofluid are independent, its capacity to store heat can be separated into two contributions

$$m_N c_N = m_P c_P + m_S c_S$$

with $^{m_P}$ and $^{c_P}$ being the mass and heat capacity of the NPs, $^{m_S}$ and $^{c_S}$ the mass and heat capacity of the solvent. Furthermore, when the NPs are capped by a lipid bilayer, then

$$m_N c_N = m_P c_P + m_S c_S + m_L c_L$$

where $^{m_L}$ and $^{c_L}$ are the mass and heat capacity of the lipid bilayer.

***Power balance equation***

The power absorbed from the laser beam is converted into heat, so the power gained by the nanofluid within the excitation cylinder is $^{W_{gain} = W_{abs}}$. This heat is then completely dissipated by the mechanisms discussed previously, so the power loss is approximated as $W_{loss}(t) \cong W_{ht}(t) + W_{UC} + W_{int}(t)$. The power balance requires that the power gained be equal to the power lost, so

$$W_{abs} = h_{ht} A_{cs} \Delta T(t) + W_{UC} + m_N c_N \frac{dT(t)}{dt} = h_{ht} A_{cs} \Delta T(t) + W_{UC} + m_N c_N \frac{d\Delta T(t)}{dt}$$

where the last equality is valid because

$$\frac{d\Delta T(t)}{dt} = \frac{d}{dt}\left[T(t) - T_0\right] = \frac{dT(t)}{dt}$$

The balance equation can be rearranged into

$$W_{abs} - W_{UC} = h_{ht}A_{cs}\Delta T(t) + m_N c_N \frac{d\Delta T(t)}{dt} \rightarrow \frac{W_{abs} - W_{UC}}{m_N c_N} = \frac{h_{ht}A_{cs}}{m_N c_N}\Delta T(t) + \frac{d\Delta T(t)}{dt}$$

or

$$B = \frac{1}{\tau}\Delta T(t) + \frac{d\Delta T(t)}{dt},\ B = \frac{W_{abs} - W_{UC}}{m_N c_N},\ \frac{1}{\tau} = \frac{h_{ht}A_{cs}}{m_N c_N}$$

The solution of this differential equation is

$$\Delta T(t) = B\tau\left(1 - e^{-t/\tau}\right)$$

for the initial condition: $\Delta T(0) = 0$.

Notice that as $t \rightarrow \infty$, the steady-state is achieved and the temperature $T(t \rightarrow \infty) = T_{ss}$ becomes the steady-state (constant) temperature and the temperature increase $\Delta T(t \rightarrow \infty) \equiv \Delta T_{ss} = T_{ss} - T_0$ is constant and given by

$$\Delta T_{ss} = T_{ss} - T_0 = B\tau = \frac{W_{abs} - W_{UC}}{m_N c_N} \frac{m_N c_N}{h_{ht}A_{cs}} = \frac{W_{abs} - W_{UC}}{h_{ht}A_{cs}} \rightarrow h_{ht}A_{cs} = \frac{W_{abs} - W_{UC}}{\Delta T_{ss}}$$

As a result,

$$\Delta T(t) = \Delta T_{ss}\left(1 - e^{-t/\tau}\right),\ \frac{1}{\tau} = \frac{h_{ht}A_{cs}}{m_N c_N} = \frac{W_{abs} - W_{UC}}{m_N c_N \Delta T_{ss}} = \frac{W_{abs}\left(1 - W_{UC}/W_{abs}\right)}{m_N c_N \Delta T_{ss}}$$

Using the approximated expression for the power absorption

$$W_{abs} \cong (N_{P,b}\sigma_P + \sigma_{S,b})P_D$$

the ratio in the numerator in the expression for $1/\tau$ becomes

$$\frac{W_{UC}}{W_{abs}} \cong \frac{0.015N_{P,b}\sigma_P P_D}{(N_{P,b}\sigma_P + \sigma_{S,b})P_D} = \frac{0.015N_{P,b}\sigma_P}{N_{P,b}\sigma_P + \sigma_{S,b}}$$

which for water solution of UCNPs is

$$\frac{W_{UC}}{W_{abs}} = \frac{0.015 \times 2.69 \times 10^8 \times 1.61 \times 10^{-19}}{2.69 \times 10^8 \times 1.61 \times 10^{-19} + 4.023 \times 10^{-9}} = \frac{6.50 \times 10^{-13}}{4.066 \times 10^{-9}} = 1.60 \times 10^{-4}$$

and for heavy water

$$\frac{W_{UC}}{W_{abs}} = \frac{0.015 \times 2.69 \times 10^8 \times 1.61 \times 10^{-19}}{2.69 \times 10^8 \times 1.61 \times 10^{-19} + 0.114 \times 10^{-9}} = \frac{6.50 \times 10^{-13}}{1.57 \times 10^{-10}} = 4.13 \times 10^{-3}$$

So, the approximations

$$\frac{1}{\tau}\cong\frac{W_{abs}}{m_N c_N \Delta T_{ss}},\ \Delta T_{ss}\cong\frac{W_{abs}}{A_{cs}h_{ht}}$$

are justified.

***Comparison between conduction and thermal radiation heat flux dissipation.***

The thermal conduction coefficients of water and dilute aqueous solutions are in the range of 500 to 900 $W\,m^{-2}\,K^{-1}$, which for $\Delta T = 10\ K$, gives a flux of heat of

$$\frac{W_{cond}}{A_{cs}} = h_{cond}\Delta T\cong\left(500-900\ W\,m^{-2}\,K^{-1}\right)(10\ K)\cong 5000-9000\ W\,m^{-2}$$

Near room temperature $T_0 = 300\ K$ and a temperature increase $\Delta T = 10\ K$, i.e. $T(t) = 310\ K$, the flux of heat dissipation by thermal radiation can be estimated as

$$\frac{W_{rad}}{A_{cs}} = \varepsilon\sigma_{SB}\left(T^4 - T_0^4\right)\cong\left(5.67\acute{}10^{-8}\ W\,m^{-2}\,K^{-4}\right)\left(310^4 - 300^4\right)\cong 64\ W\,m^{-2}$$

Thus, under the experimental conditions, the heat dissipation by thermal radiation is negligible compared to heat dissipation by conduction.

## VI. Temperature variations within the excitation cylinder

It is relevant to determine how the temperature increase, $\Delta T$, associated with absorption, varies across and along with the excitation cylinder of the laser beam. These variations of $\Delta T$ will determine the accuracy and reliability of the derived properties as well as establish the temperature monitoring.

***Temperature variation across a cylinder at steady-state***

At steady-state, the energy stored due to heat capacity is constant, so the rate of internal energy variation is null. As discussed previously, the only source of heat dissipation is via conduction. In addition, at steady-state: $T(r,t) = T(r)$ and $\dot{Q}_{cond}(r,t) = \dot{Q}_{cond}(r)$. The heat

generated within an inner excitation cylinder must be equal to the heat conducted through its outer surface. Assuming constant thermal conductivity, $\kappa(r,T) = \kappa$, conservation of energy requires that

$$\dot{Q}_{cond}(r) = -\kappa A_r \frac{dT(r)}{dr} = \dot{E}_{gen} = \dot{e}_{gen} V_r$$

where $\dot{E}_{gen}$ and $\dot{e}_{gen}$ are the rate of energy and the rate of energy density generated within the cylinder with a surface area $A_r = 2\pi rL$ and volume $V_r = \pi r^2 L$, which gives

$$-\kappa(2\pi rL)\frac{dT(r)}{dr} = \dot{e}_{gen}(\pi r^2 L) \rightarrow \frac{dT(r)}{dr} = -\frac{\dot{e}_{gen}}{2\kappa} r$$

Separating the variables and integrating from $r = 0$ for which $T(0) = T_0$ to the surface $r = R_s$ where $T(R_s) = T_s$, then

$$\int_{T_0}^{T_s} dT = -\frac{\dot{e}_{gen}}{2\kappa} \int_0^{R_s} r dr \rightarrow \Delta T = T_{surface} - T_{center} = -\frac{\dot{e}_{gen} r^2}{2\kappa\ 2}\Big|_0^{R_s} = -\frac{\dot{e}_{gen}}{4\kappa} R_s^2$$

For heating with a laser beam with spot area, $A_b$, and pathlength, $L$, the rate of energy density generation becomes $\dot{e}_{gen} = \dot{E}_{gen}/V_b = \dot{E}_{gen}/(A_b L)$. Considering that the power absorbed from the laser beam is converted in heat, then as shown previously, the rate of energy generation becomes $W_{abs}$, that is, $\dot{E}_{gen} = -W_{abs}$, which gives the following temperature variation across the laser beam

$$\Delta T = T_{surface} - T_{center} = \frac{W_{abs}}{4\kappa A_b L} R_s^2$$

Thus, with $R_s = R_b$ and $A_b = \pi R_b^2$, the temperature variation across the laser beam is

$$\Delta T = T_{surface} - T_{center} = \frac{W_{abs}}{4\kappa\pi R_b^2 L} R_b^2 = \frac{W_{abs}}{4\pi\kappa L} = \frac{\left(1 - e^{-\alpha_N L}\right) A_b P_D}{4\pi\kappa L} \cong \frac{(N_{P,b}\sigma_P + \sigma_S) P_D}{4\pi\kappa L}$$

This temperature variation can be estimated as

$$\Delta T = \frac{\left(1 - e^{-\alpha L}\right) A_b P_D}{4\pi\kappa L} = \frac{\left(1 - e^{-0.502}\right)\left(8.01 \cdot 10^{-9}\, m^2\right)\left(1.50 \times 10^6\, W\, m^{-2}\right)}{4\pi\left(0.615\, W\, m^{-1}\, K^{-1}\right)\left(10^{-2}\, m\right)} = 0.061\, K$$

where typical values for water or dilute aqueous solutions were used, namely, $\alpha = 0.502\ cm^{-1}$ (water at 980 nm), $L = 1.00\ cm$, $A_b = 8.01 \cdot 10^{-9}\ m^2$, $\kappa = 0.615\ W\ m^{-1}\ K^{-1}$ (water at 300 K), and $P_D = 150\ W\ cm^{-2}$. Therefore, the temperature can be considered uniform across the laser beam.

***Temperature variation along a cylinder defined by the laser beam***

It was shown that the energy rate, $dW_{abs}$, absorbed in an infinitesimal segment $dx$ is

$$dW_{abs} = \alpha_N P_D dV_b = A_b \alpha_N P_D dx = A_b \alpha_N P_{D,0} e^{-\alpha_N x} dx$$

Thus, the absorbed power, $W_{abs}(x_1,x_2)$, in a segment $(x_1,x_2)$ of the optical path is

$$W_{abs}(x_1,x_2) = A_b \alpha_N P_{D,0} \int_{x_1}^{x_2} e^{-\alpha_N x} dx = -A_b P_{D,0} e^{-\alpha_N x}\Big|_{x_1}^{x_2} = A_b P_{D,0}\left(e^{-\alpha_N x_1} - e^{-\alpha_N x_2}\right)$$

The power balance equation for this segment of absorbed energy rate requires that

$$W_{abs}(x_1,x_2) = A_b P_D\left(e^{-\alpha_N x_1} - e^{-\alpha_N x_2}\right) = mc\frac{dT(t)}{dt} + h_{cond} A_{1,2} \Delta T(t)$$

where $m$ is the mass, $c$ is the heat capacity, $h_{cond}$ is the thermal conductivity coefficient (in $W\ m^{-2}\ K^{-1}$), and $A_{1,2}$ is the surface area of the cylinder segment $(x_1,x_2)$ given by

$$A_{1,2} = 2\pi R_b (x_2 - x_1)\left[1 + \frac{R_b}{(x_2 - x_1)}\right]$$

So,

$$\frac{d\Delta T(t)}{dt} + \frac{h_{cond} A_{1,2}}{mc}\Delta T(t) - \frac{A_b P_D\left(e^{-\alpha_N x_1} - e^{-\alpha_N x_2}\right)}{mc} = 0$$

or

$$\frac{dy(t)}{dt} + \frac{1}{\tau_{1,2}} y(t) - B_{1,2} = 0$$

where

$$\frac{1}{\tau_{1,2}} = \frac{h_{cond} A_{1,2}}{mc},\ B_{1,2} = \frac{A_b P_D\left(e^{-\alpha_N x_1} - e^{-\alpha_N x_2}\right)}{mc}$$

The solution is

$$\Delta T_{1,2}(t) = B_{1,2}\tau_{1,2}\left(1 - e^{-t/\tau_{1,2}}\right)$$

for the initial condition: $\Delta T(0) = 0$. Similarly, for the interval cylinder segment $(x_3, x_4)$.

Then,

$$\frac{\Delta T_{1,2}(t)}{\Delta T_{3,4}(t)} = \frac{B_{1,2}\tau_{1,2}\left(1 - e^{-t/\tau_{1,2}}\right)}{B_{3,4}\tau_{3,4}\left(1 - e^{-t/\tau_{3,4}}\right)}$$

In addition,

$$\frac{B_{1,2}}{B_{3,4}} = \frac{\frac{A_b P_D\left(e^{-\alpha_N x_1} - e^{-\alpha_N x_2}\right)}{mc}}{\frac{A_b P_D\left(e^{-\alpha_N x_3} - e^{-\alpha_N x_4}\right)}{mc}} = \frac{\left(e^{-\alpha_N x_1} - e^{-\alpha_N x_2}\right)}{\left(e^{-\alpha_N x_3} - e^{-\alpha_N x_4}\right)}$$

and

$$\frac{\tau_{1,2}}{\tau_{3,4}} = \frac{\frac{mc}{h_{cond}A_{1,2}}}{\frac{mc}{h_{cond}A_{3,4}}} = \frac{A_{3,4}}{A_{1,2}}$$

Choosing the same interval lengths, that is, $(x_2 - x_1) = (x_3 - x_4)$, then $A_{1,2} = A_{3,4}$, and the ratio of temperature increases becomes

$$\frac{\Delta T_{1,2}(t)}{\Delta T_{3,4}(t)} = \frac{B_{1,2}\tau_{1,2}\left(1 - e^{-t/\tau_{1,2}}\right)}{B_{3,4}\tau_{3,4}\left(1 - e^{-t/\tau_{3,4}}\right)} = \frac{\left(e^{-\alpha_N x_1} - e^{-\alpha_N x_2}\right)\left(1 - e^{-t/\tau_{1,2}}\right)}{\left(e^{-\alpha_N x_3} - e^{-\alpha_N x_4}\right)\left(1 - e^{-t/\tau_{3,4}}\right)}$$

In the first instants of the transient regime $t/\tau \ll 1$, so

$$1 - e^{-t/\tau} = 1 - \left[1 - \frac{t}{\tau} + \frac{1}{2}\left(\frac{t}{\tau}\right)^2 - \cdots\right] \cong \frac{t}{\tau}$$

then,

$$\frac{\Delta T_{1,2}(t)}{\Delta T_{3,4}(t)} \cong \frac{\left(e^{-\alpha_N x_1} - e^{-\alpha_N x_2}\right)t/\tau_{1,2}}{\left(e^{-\alpha_N x_3} - e^{-\alpha_N x_4}\right)t/\tau_{3,4}} \cong \frac{\left(e^{-\alpha_N x_1} - e^{-\alpha_N x_2}\right)\tau_{3,4}}{\left(e^{-\alpha_N x_3} - e^{-\alpha_N x_4}\right)\tau_{1,2}} = \frac{\left(e^{-\alpha_N x_1} - e^{-\alpha_N x_2}\right)}{\left(e^{-\alpha_N x_3} - e^{-\alpha_N x_4}\right)}$$

because the segments have the same areas, $A_{1,2} = A_{3,4}$, so $\tau_{3,4}/\tau_{1,2} = 1$.

As $t \to \infty$, steady-state is achieved and the ratio between the temperature increase in each segment is the same as that calculated for the first instants of the transient regime:

$$\frac{\Delta T_{1,2}(t)}{\Delta T_{3,4}(t)} = \frac{B_{1,2}\tau_{1,2}\left(1 - e^{-t/\tau_{1,2}}\right)}{B_{3,4}\tau_{3,4}\left(1 - e^{-t/\tau_{3,4}}\right)} = \frac{B_{1,2}\tau_{1,2}}{B_{3,4}\tau_{3,4}} = \frac{B_{1,2}}{B_{3,4}} = \frac{\left(e^{-\alpha_N x_1} - e^{-\alpha_N x_2}\right)}{\left(e^{-\alpha_N x_3} - e^{-\alpha_N x_4}\right)},\ t \to \infty$$

Thus, the ratio between the temperature increase in each segment at the first instants of the transient or steady-state regimes becomes independent of time:

$$\frac{\Delta T_{1,2}(t)}{\Delta T_{3,4}(t)} \cong \frac{\left(e^{-\alpha_N x_1} - e^{-\alpha_N x_2}\right)}{\left(e^{-\alpha_N x_3} - e^{-\alpha_N x_4}\right)}$$

For $\alpha_N = 0.50\ cm^{-1}$, $x_1 = 0$, $x_2 = 0.1L = 0.1\ cm$, $x_3 = 0.9L = 0.9\ cm$, and $x_4 = L = 1\ cm$, then

$$\frac{\Delta T_{1,2}(t)}{\Delta T_{3,4}(t)} \cong \frac{\left(e^{-0} - e^{-0.05}\right)}{\left(e^{-0.45} - e^{-0.50}\right)} = \frac{(1 - 0.9512)}{(0.6376 - 0.6065)} = \frac{0.0488}{0.0311} = 1.57$$

This result indicates that the temperature increase, $\Delta T$, in the last segment ($0.9L - 1.0L$) of the optical pathlength becomes *ca.* 1.6 times smaller than that in the first segment ($0 - 0.1L$). Or, the temperature increase, $\Delta T$, due to laser excitation decreases monotonically along the optical pathlength as shown in Figure S3.

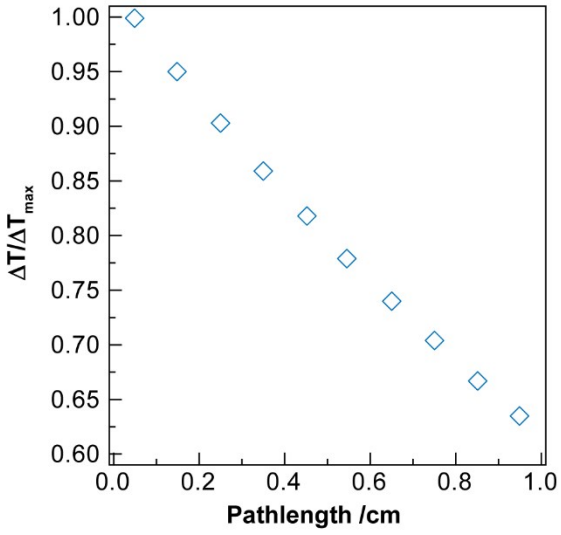


**Figure S3.** Variation of the temperature increase, ΔT, due to laser excitation along the pathlength.

Therefore, it is very important, for quantitative measurements, to ensure that the temperature is monitored at the same position along the cylinder defined by the laser beam for all samples. This is the main reason that temperature monitoring by ratiometric luminescence at each UCNP will not be addressed in these experiments. However, because the size of the thermocouple (*ca.* 1.5 mm = 0.15 cm) is small, there is a little variation (< 4%) of $\Delta T$ cross the excitation cylinder of the laser beam, so $\Delta T$ monitored by the thermocouple can be considered uniform.

Centering the thermocouple at the middle of the pathlength (*e.g.* $0.5\ cm$), using $\alpha_N = 0.50\ cm^{-1}$ and $L = 1\ cm$: $\alpha_N x_1 = 0.50 \cdot 0.425 = 0.2125$, $\alpha_N x_2 = \alpha_N x_3 = 0.50 \cdot 0.5 = 0.25$, and $\alpha_N x_4 = 0.50 \cdot 0.575 = 0.2875$, then

$$\frac{\Delta T_{1,2}(t)}{\Delta T_{3,4}(t)} \cong \frac{\left(e^{-0.2125} - e^{-0.25}\right)}{\left(e^{-0.25} - e^{-0.2875}\right)} = 1.0382 \rightarrow 3.82\%$$

## VII. Analysis

The analysis of transient regime yields the following expression for the heat capacity, $c_N$, of the nanofluid

$$c_N = \frac{W_{abs}\tau}{\Delta T_{ss} m_N},\ W_{abs} = \sigma_N P_D = (N_{P,b}\sigma_P + N_{P,b}\sigma_L + \sigma_S)P_D$$

where the power absorbed, $W_{abs}$, from the laser beam can be determined from its power density, $P_D$, and the absorption cross-section of the nanofluid, $\sigma_N = N_{P,b}\sigma_P + N_{P,b}\sigma_L + \sigma_S$, whereas the temperature increase at the steady-state, $\Delta T_{ss}$, can be measured and the time associated with the transient regime, $\tau$, can be determined by fitting the temperature increase with time. It is noteworthy that the determination of the heat capacity, $c_N$, is independent of the thermal conduction coefficient, $h_{cond}$, and of the cross-sectional area of heat flux, $A_{cs}$.

From the dependence of $\Delta T_{ss}$ on the laser power density, $P_D$,

$$h_{ht} \cong \frac{W_{abs}}{A_{cs}\Delta T_{ss}},\ W_{abs} = \sigma_N P_D = (N_{P,b}\sigma_P + N_{P,b}\sigma_L + \sigma_S)P_D$$

it is possible to determine the conduction heat transfer coefficient, $h_{ht}$, using values of $\sigma_N$ and $A_{cs}$. As mentioned, under the experimental conditions, this heat transfer coefficient, $h_{ht}$, is basically the conduction heat transfer coefficient, $h_{cond}$. As the thermal conductivity, $\kappa_m$, and $h_{cond}$ are related: $\kappa_m = h_{cond}\Delta r$, the values obtained for $h_{cond}$ with the present analysis agree with the thermal conductivities previously reported.[2] The only difference was that in this previous work the absorption of $D_2O$ was neglected compared to that of uncapped UCNPs.[2] However, the contribution of $D_2O$ was to be taken into account because its absorption coefficient at 980 nm (1.42 $m^{-1}$ [3]) is higher than those of capped (0.8180±0.0001 $m^{-1}$) and uncapped (0.5400±0.0001 $m^{-1}$) UCNPs.

The determination of $\Delta T_{ss}$ is straightforward and it is related to the thermal conduction properties of the nanofluid. However, care must be exercised in the determination of $\tau$. For

instance, the direct fit of the curve $\Delta T(t) = \Delta T_{ss}(1 - e^{-t/\tau})$ will be dominated by the steady-state region, so the time of temperature increase during the transient regime will not be properly adjusted, as can be observed in Figure S4a. Alternatively, this curve can be linearized as

$$\theta(t) \equiv \frac{\Delta T(t)}{\Delta T_{ss}} = 1 - e^{-t/\tau} \rightarrow \ln[1 - \theta(t)] = -\frac{1}{\tau}t$$

so, $\tau$ can be obtained from the inverse of the slope of the linear region of the plot $\ln[1 - \theta(t)]$ vs. $t$, as observed in Figure S4b. For pure water, the heat capacity can be determined as

$$c_{H_2O} = \frac{\sigma_{H_2O} P_D \tau}{\Delta T_{ss} m_{H_2O}}$$

and presented in Table S1.

**Table S1.** Fitting parameters for pure water at several laser power densities.

| $P_D$ **(**$10^6\ W\ m^{-2}$**)** | $\Delta T_{ss}$ **(**$\pm\ 0.1\ K$**)** | $\tau$ **(s)** | $c_{H_2O}$ **(**$J\ kg^{-1}\ K^{-1}$**)**[a)] |
|---|---|---|---|
| 1.49 | 5.1 | 0.28±0.02 | |
| 1.97 | 6.8 | 0.29±0.02 | 4177±367 |
| 2.22 | 8.2 | 0.31±0.01 | |

[a)] determined with $\sigma_{H_2O} = (4.023 \pm 0.005) \times 10^{-9}\ m^2$ and $m_{H_2O} = (7.99 \pm 0.01) \times 10^{-8} kg$.

The values of $\tau$ were obtained from fitting the measured temperature increase in the first instants of the transient regime, that is, the linear region of the plot $\ln[1 - \theta(t)]$ vs. $t$, as illustrated in Figure S4b.

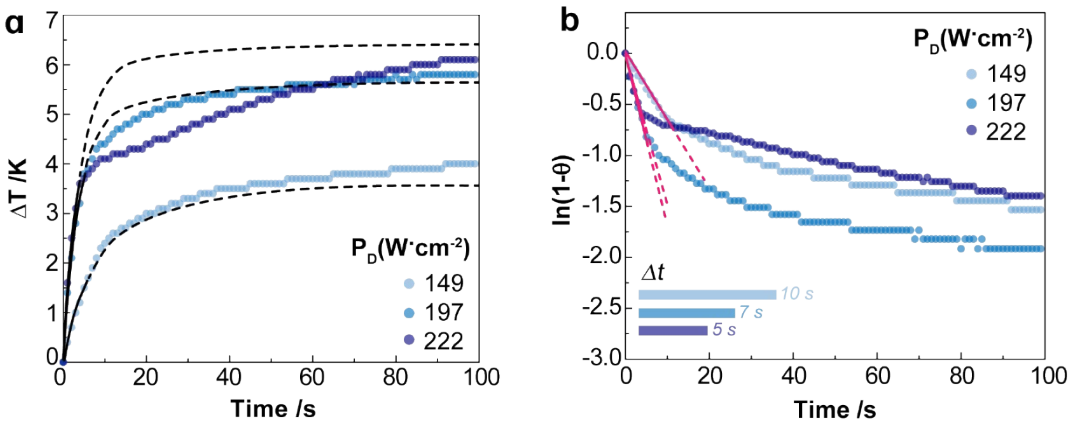


**Figure S4.** (a) Temperature increase, $\Delta T(t)$, with time for pure water. (b) Temporal dependence of the logarithm of $1-\theta(t)$, where $\theta(t)$ is the reduced temperature $\theta(t) = \Delta T(t)/\Delta T_{ss}$.

## VIII. Absorption spectroscopy

The absorption spectra were recorded three times at room temperature, using a dual-beam spectrometer Lambda 950 (Perkin-Elmer) with a 150 mm diameter Spectralon integrating sphere over the range 200-1200 nm with a resolution of 1.0 nm. A baseline was recorded with two 10 mm path-length quartz cuvettes (2 polished windows) containing the reference fluid ($H_2O$). The absorbance uncertainty (~$10^{-6}$) was estimated through the resolution of the device and the maximum deviation between the three measurements performed for the same sample. Following the equation for the absorption coefficient, $\alpha$ (in $m^{-1}$),

$$\alpha = \frac{A}{L}$$

where $A$ is the absorbance of the UCNPs at 980 nm using the solvent as the reference and $L$ is the optical pathlength ($0.0100 \pm 0.0001\ m$), the uncertainty in $\alpha$ is estimated as:

$$\Delta\alpha = \sqrt{\left(\frac{\Delta A}{L}\right)^2 + \left(\frac{A}{L^2}\Delta L\right)^2}.$$

## IX. Photoluminescence in the NIR spectral range

Photoluminescence spectra in the NIR spectral range were measured using the Quantaurus-QY (C13534, Hamamatsu) system equipped with an integrating sphere as sample chamber and two multi-channel analyzers for signal detection in the visible and the NIR spectral ranges. A 980 nm external laser diode (FC-980 5W, CNI Lasers) was used as the excitation source (operating at ~2.4 W, corresponding to $P_D$=950 W·cm$^{-2}$, considering the illumination area in the sample holder, 0.0025 cm2, according to the manufacturer). The emission spectra of the UCNPs upon 980 nm excitation display the $^2H_{11/2}$,$^4S_{3/2}\rightarrow{}^4I_{15/2}$ (green spectral region) and $^4F_{9/2}\rightarrow{}^4I_{15/2}$ (red spectral region) $Er^{3+}$ transitions, Figure S5.

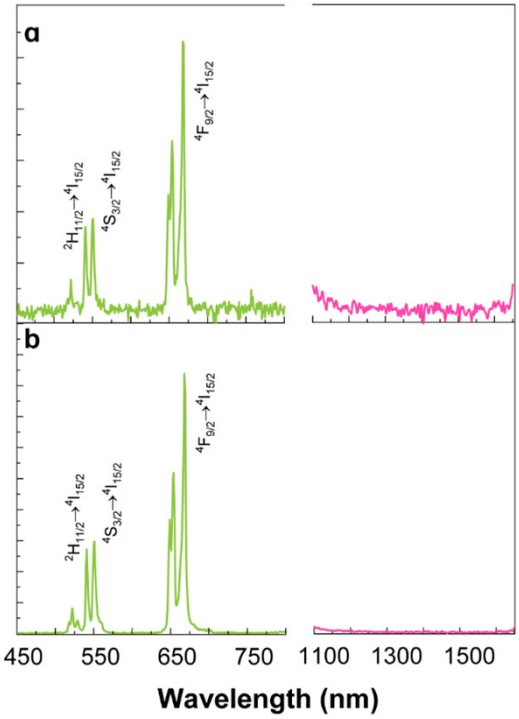


**Figure S5.** Emission spectra of the (a) uncapped and (b) lipid bilayer-capped $LiYF_4$:$Yb^{3+}$/$Er^{3+}$ UCNPs dispersed in $H_2O$ recorded between 450 and 1600 nm upon 980 nm excitation. The $Er^{3+}$ emission in the near-infrared spectral region is not detected indicating that the 980 nm excitation is essentially converted in upconversion emission and, thus, the $Er^{3+}$ downshifting emission is negligible.

## X. Supplementary Tables

**Table S2.** Properties of uncapped $LiYF_4:Er^{3+}/Yb^{3+}$ UCNPs and lipid bilayer capped $LiYF_4:Er^{3+}/Yb^{3+}$ UCNPs.

| | Quantity | Value | Units |
|---|---|---|---|
| **Uncapped UCNPs** | Average molar mass ($LiYF_4$:Er 0.6%/Yb 29%), $M_P$ | 0.19671 | $kg{\cdot}mol^{-1}$ |
| | Size of long diagonal, $d_l$ | 86.4±9.5 | nm |
| | Size of small diagonal, $d_s$ | 52.2±5.3 | nm |
| | Volume of one UCNP, $V_P$ | 3.92±1.2 | $10^{-23}\,m^3$ |
| | Density of undoped $LiYF_4$, $\rho_{LiYF_4}$ | 3995±5[4] | $kg{\cdot}m^{-3}$ |
| | Mass of one UCNP, $m_P$ | 1.79±0.6 | $10^{-19}\,kg$ |
| **Capped UCNPs** | Average molar mass lipid bilayer capped UCNP (Oleate 20%: DOPA 51%: DOPC 5%: Chol 24%), $M_{cP}$ | 0.58167 | $kg{\cdot}mol^{-1}$ |
| | Thickness of lipid bilayer | 4.40±0.40[5] | nm |
| | Mass of one lipid bilayer, $m_L$ | 0.53 ±0.08 | $10^{-19}\,kg$ |
| | Mass of one lipid bilayer-UCNP composite, $m_{cP}$ | 2.32 ±0.64 | $10^{-19}\,kg$ |
| | Volume one lipid bilayer-UCNP composite, $V_{cP}$ | 4.85±1.51 | $10^{-23}\,m^3$ |

**Table S3.** Properties of the nanofluids. Uncapped UCNPs = UCNPs and lipid bilayer-UCNP = c-UCNPs.

| Quantity | Value | Units |
|---|---|---|
| Concentration of UCNPs, $C_P$, and c-UCNPs, $C_{cP}$ | 0.6 | $g{\cdot}L^{-1}$ |
| Number density of UCNPs, $N_P$ | 3.35±1.05 | $10^{18}\,NPs\,m^{-3}$ |
| Number density of c-UCNPs, $N_{cP}$ | 2.59±0.72 | |
| Number of UCNPs exposed to the laser beam, $N_{P,b}$ | 2.69±0.85 | $10^8$ |
| Number of c-UCNPs exposed to the laser beam, $N_{cP,b}$ | 2.07±0.58 | |
| Absorption coefficient of UCNPs, $\alpha_P$ | 0.540±0.005 | $m^{-1}$ |
| Absorption coefficient of c-UCNPs, $\alpha_{cP}$ | 0.818±0.009 | $m^{-1}$ |
| Absorption cross-section of UCNP, $\sigma_P$ | 1.61±0.52 | |
| Absorption cross-section of lipid bilayer, $\sigma_L$ | 1.55±0.35 | $10^{-19}{\cdot}m^2$ |
| Absorption cross-section of c-UCNP, $\sigma_{cP}$ | 3.16±0.82 | |

**Table S4.** Properties of the solvents at 298 K.

| Parameter | $H_2O$ | $D_2O$ | Units |
|---|---|---|---|
| Molar mass, $M_S$ | 0.018015 | 0.02003 | $kg{\cdot}mol^{-1}$ |
| Mass density, $\rho_S$ | 997[6] | 1104[7] | $kg{\cdot}m^{-3}$ |
| Absorption coefficient, $\alpha_S$ | 50.2[8] | 1.42[3] | $m^{-1}$ |
| Absorption cross-section within the laser beam | 4.023±0.005 | 0.114±0.001 | $10^{-9}\,m^2$ |

**Table S5.** Physical parameters of the experimental set-up.

| Parameter | Value | Units |
|---|---|---|
| Wavelength | 980 | $10^{-9}$ m |
| Cuvette pathlength, $L$ | 10.0±0.1 | ×$10^{-3}$ m |
| Laser beam spot area, $A_b$ | 8.01±0.01[2] | $10^{-9}\,m^2$ |
| Cross-sectional area, $A_{cs}$ | 3.19±0.05 | $10^{-6}\,m^2$ |

**Table S6.** Fitting parameters for the uncapped $LiYF_4$:$Er^{3+}$/$Yb^{3+}$ UCNPs dispersed in $D_2O$ for several laser power densities.

| $P_D$ **(**$10^6\,W{\cdot}m^{-2}$**)** | $\Delta T_{ss}$ **(**$\pm 0.1\,K$**)** | $\tau$ **(s)** | $c_P$ **(**$J{\cdot}kg^{-1}{\cdot}K^{-1}$**)** [a)] |
|---|---|---|---|
| 1.25 | 1.5 | 2.88±0.23 | 709±93 |
| 2.22 | 3.9 | 4.21±0.39 | |

[a)] determined with $\sigma_{D_2O} = (0.114 \pm 0.001) \times 10^{-9}\,m^2$, $\sigma_P = (1.61 \pm 0.52) \times 10^{-19}\,m^2$, $N_{P,b} = (2.69 \pm 0.85) \times 10^8$, $m_{D_2O} = (8.87 \pm 0.01) \times 10^{-8}\,kg$, $c_{D_2O} = 4219\,J\,kg^{-1}\,K^{-1}$, and $m_P = (4.81 \pm 2.14) \times 10^{-11}\,kg$.

$c_N = \frac{W_{abs}\tau}{\Delta T_{ss} m_N}$, $W_{abs} = \sigma_N P_D = (N_{P,b}\sigma_P + N_{P,b}\sigma_L + \sigma_S)P_D$

$W_{abs} = \left(2.69 \times 10^8 \times 1.61 \times 10^{-19} + 0.114 \times 10^{-9}\right)P_D = 1.573 \times 10^{-10} P_D$

**Table S7.** Fitting parameters for the uncapped $LiYF_4$:$Er^{3+}$/$Yb^{3+}$ UCNPs dispersed in $H_2O$ for several laser power densities.

| $P_D$ **(**$10^6\,W{\cdot}m^{-2}$**)** | $\Delta T_{ss}$ **(**$\pm 0.1\,K$**)** | $\tau$ **(s)** | $c_P$ **(**$J{\cdot}kg^{-1}{\cdot}K^{-1}$**)** [a)] |
|---|---|---|---|
| 1.25 | 5.0 | 0.33±0.02 | 715±57 |
| 1.49 | 7.1 | 0.39±0.01 | |
| 1.97 | 7.9 | 0.33±0.01 | |
| 2.22 | 13.8 | 0.51±0.03 | |

[a)] determined with $\sigma_{H_2O} = (4.023 \pm 0.005) \times 10^{-9}\, m^2$, $\sigma_P = (1.61 \pm 0.52) \times 10^{-19}\, m^2$, $N_{P,b} = (2.69 \pm 0.85) \times 10^{8}$, $m_{H_2O} = (7.99 \pm 0.01) \times 10^{-8}\, kg$, $c_{H_2O} = 4184\, J\, kg^{-1}\, K^{-1}$ [9], and $m_P = (4.81 \pm 2.14) \times 10^{-11} kg$.

**Table S8.** Fitting parameters for the lipid bilayer capped $LiYF_4:Er^{3+}/Yb^{3+}$ UCNPs dispersed in $H_2O$ for several power densities.

| $P_D$ **(**$10^6\ W{\cdot}m^{-2}$**)** | $\Delta T_{ss}$ **(**$\pm 0.1\ K$**)** | $\tau$ **(s)** | $c_L$ **(**$J{\cdot}kg^{-1}{\cdot}K^{-1}$**)** [a] |
|---|---|---|---|
| 0.67 | 3.6 | 0.44±0.01 | 5039±211 |
| 0.95 | 4.9 | 0.42±0.01 | |
| 1.25 | 5.2 | 0.34±0.02 | |
| 1.49 | 9.7 | 0.54±0.03 | |
| 1.97 | 10.9 | 0.46±0.02 | |
| 2.22 | 16.2 | 0.60±0.03 | |

[a] determined with $\sigma_{H_2O} = (4.023 \pm 0.005) \times 10^{-9}\ m^2$, $\sigma_{cP} = (3.16 \pm 0.82) \times 10^{-19}\ m^2$, $N_{cP,b} = (2.07 \pm 0.58) \times 10^8$, $m_{H_2O} = (7.99 \pm 0.01) \times 10^{-8}\ kg$, $c_{H_2O} = 4184\ J{\cdot}kg^{-1}{\cdot}K^{-1}$ [9], $m_P = (3.71 \pm 1.56) \times 10^{-11}\ kg$, $c_P = (715 \pm 57)\ J{\cdot}kg^{-1}{\cdot}K^{-1}$, and $m_L = (1.10 \pm 0.47) \times 10^{-11}\ kg$.

## XI. References


1. T. L. Bergman, A. S. Lavine, F. P. Incropera and D. P. DeWitt, *Fundamentals of Heat and Mass Transfer*, Wiley, New York, 7 edn., 2011.
2. A. R. N. Bastos, C. D. S. Brites, P. A. Rojas-Gutierrez, C. DeWolf, R. A. S. Ferreira, J. A. Capobianco and L. D. Carlos, *Adv. Funct. Mater.*, 2019, **29**, 1905474.
3. S. Kedenburg, M. Vieweg, T. Gissibl and H. Giessen, *Opt. Mater. Express*, 2012, **2**, 1588-1611.
4. W. A. Shand, *J. Cryst. Growth*, 1969, **5**, 143-146.
5. P. A. Rojas-Gutierrez, C. DeWolf and J. A. Capobianco, *Part. Part. Syst. Char.*, 2016, **33**, 865-870.
6. M. L. Huber, R. A. Perkins, D. G. Friend, J. V. Sengers, M. J. Assael, I. N. Metaxa, K. Miyagawa, R. Hellmann and E. Vogel, *J. Phys. Chem. Ref. Data*, 2012, **41**, 033102.
7. A. Blahut, J. Hykl, P. Peukert, V. Vins and J. Hruby, *J. Chem. Phys.*, 2019, **151**, 034505.
8. K. F. Palmer and D. Williams, *J. Opt. Soc. Am.*, 1974, **64**, 1107-1110.
9. W. M. Haynes, *CRC Handbook of Chemistry and Physics*, CRC Press, Boca Raton, FL, 2017.